Chemosphere 93 (2013) 230–237

Contents lists available at SciVerse ScienceDirect

Chemosphere

journal homepage: www.elsevier.com/locate/chemosphere

Effects of cadmium on the activities of photosystems of *Chlorella pyrenoidosa* and the protective role of cyclic electron flow

Shuzhi Wang [a,b], Daoyong Zhang [c,*], Xiangliang Pan [a,*]

[a] Laboratory of Environmental Pollution and Bioremediation, Xinjiang Institute of Ecology and Geography, Chinese Academy of Sciences, Urumqi 830011, China
[b] University of Chinese Academy of Sciences, Beijing 100049, China
[c] State Key Laboratory of Environmental Geochemistry, Institute of Geochemistry, Chinese Academy of Sciences, Guiyang 550002, China

HIGHLIGHTS

- Effects of $CdCl_2$ on PSI, PSII activities and CEF in *Chlorella pyrenoidosa* was studied.
- CEF was stimulated by Cd and played an essential role for the protection of PSI.
- PSII was more sensitive to Cd treatment than PSI.

ARTICLE INFO

Article history:
Received 11 September 2012
Received in revised form 13 February 2013
Accepted 21 April 2013
Available online 30 May 2013

Keywords:
Cadmium
Photosystem I
Photosystem II
Cyclic electron flow
Chlorella pyrenoidosa

ABSTRACT

Cadmium (Cd) shows high toxicity to aquatic microalgae. Many studies showed that Cd inhibited activities of photosystem II (PSII) but the effects of heavy metals on photosystem I (PSI) and cyclic electron flow (CEF) were still controversial and unclear. The effects of $CdCl_2$ on the activities of PSI, PSII and CEF in *Chlorella pyrenoidosa* was measured simultaneously in the present study. In presence of 200 μM of Cd, ultrastructure of some cells was strongly modified. Cd exposure led to decrease of the activities of photosynthetic oxygen evolution and respiration. PSII was more sensitive to Cd treatment than PSI. Cd treatment showed significant inhibition on the photochemical quantum yield and electron transport rate of PSII. Cd increased the quantum yield of non-light-induced non-photochemical fluorescence quenching, indicating the damage of PSII. The activity of PSI showed tolerance to Cd treatment with concentration less than 100 μM in the experiment. Linear electron flow (LEF) made significant contribution to the photochemical quantum yield of PSI of the untreated cells, but decreased with increasing Cd concentration. The contribution of CEF to the yield of PSI increased with increasing Cd concentration. The activation of CEF after exposure to Cd played an essential role for the protection of PSI.

1. Introduction

Heavy metal pollution is one of the most important environmental problems today and increasing continuously as a result of industrial activities and technological development (Wang and Chen, 2009). Heavy metal contamination poses serious threat to the environment and human health. Cadmium (Cd) is considered as one of the major metal pollutants because of its wide distribution in aquatic ecosystems and its high toxicity (Nawrot et al., 2006; Zhou et al., 2006; Monteiro et al., 2011). It is not essential for life and extremely toxic to humans, animals and plants (Chen et al., 1999; Khattar and Shailza, 2009; Qian et al., 2009). It shows more serious toxicity to plants or algae than some other heavy metals or pesticides.

Effects of heavy metals on phytoplankton species including cyanobacteria have been extensively studied (Silverberg, 1976; Fargašová et al., 1999; Kola and Wilkinson, 2005). Phytoplankton species like cyanobacteria or green alga are also widely used as experimental materials to estimate the risk of heavy metals or other contaminants in aquatic systems (Qian et al., 2009; Wang and Pan, 2012). Many studies showed that heavy metals inhibited activities of photosystem II (PSII), which was suggested to be one of the sensitive target sites for environmental stress (Dewez et al., 2005; Perales-Vela et al., 2007; Pan et al., 2009). Exposure to heavy metals could lead to inhibition of capture and transfer of energy, quantum yield of photochemistry of PSII, and the synthesis of chlorophyll (Dewez et al., 2005; Zhang et al., 2010). Cd is thought to have toxicity to PSII by acting on the donor side or the acceptor side or inhibiting activity of oxygen-evolving complex (Atal et al., 1991; Siedlecka and Krupa, 1996; Zhou et al., 2006). A few studies investigated the relationship between heavy metals and the activity of photosystem I (PSI), showing that the effects of heavy metals

* Corresponding authors. Tel./fax: +86 991 7885446.
E-mail addresses: zhang-daoyong@163.com (D. Zhang), panxl@ms.xjb.ac.cn (X. Pan).

0045-6535/$ - see front matter © 2013 Elsevier Ltd. All rights reserved.
http://dx.doi.org/10.1016/j.chemosphere.2013.04.070

on PSI were still controversial and unclear (Neelam and Rai, 2003; Zhou et al., 2006). Neelam and Rai (2003) found that Cd inhibited PSI activity in *Microcystis* sp. However, Zhou et al. (2006) reported that the activity of PSI in *Microcystis aeruginosa* increased due to Cd treatment.

The noninvasive chlorophyll fluorescence measurements can provide valuable information about the response of PSII to environmental stress (Appenroth et al., 2001; Pan et al., 2009). Although many studies investigated the effects heavy metals on PSII, toxicity of heavy metals to PSI and PSII has been rarely analyzed simultaneously. The simultaneous measurement of the photosynthetic activities of PSI and PSII are necessary to detect the effects of heavy metals on photosynthetic apparatus and the relation between PSII and PSI under stress. Klughammer and Schreiber (1994) introduced an improved method for the determination of PSI quantum yield and a Dual-PAM-100 system, which can simultaneously detect the chlorophyll fluorescence and $P700^+$ absorbance changes. Many studies have shown that the Dual-PAM-100 system becomes a powerful tool for investigation of response of PSI and PSII to environmental stress (Coopman et al., 2010; Huang et al., 2010).

The cyclic electron flow (CEF) around PSI was important for photoprotection and photosynthesis (Munekage et al., 2004; Suzuki et al., 2011), and the increase of CEF around PSI was suggested be one of the adaptive mechanisms to heavy metal stress (Zhou et al., 2006; Qian et al., 2009). However, effects of heavy metals like cadmium on CEF in green algae were still unclear.

In the present study, the activities of PSI, PSII and CEF in *Chlorella pyrenoidosa* was measured simultaneously to detect the quantum yields, electron transport and energy dissipation in PSI and PSII, and the relation between PSI and PSII under Cd treatment. In addition, toxic effects of $CdCl_2$ on the cell structure, photosynthetic oxygen development and respiration were tested.

2. Materials and methods

2.1. Culture of C. pyrenoidosa

C. pyrenoidosa (FACHB-9) was purchased from Freshwater Algae Culture Collection of Institute of Hydrobiology, Chinese Academy of Sciences (Wuhan, China), and cultured in BG-11 medium (Stanier et al., 1971) at 25 °C under fluorescent white light (30 μmol photons $m^{-2}\,s^{-1}$) with a 12:12 h light–dark cycle. The cells in exponential growth phase were harvested for the following experiment by testing the growth state of cultures every day by measuring cell optical density at 680 nm (OD_{680}) with a UV2800 spectrophotometer (Unico, Shanghai, China).

2.2. Treatments

Exponentially grown cells used for different treatments were harvested and cultured in 50 mL flasks with 25 mL of BG-11 medium or prepared Cd solutions to make the final Cd concentrations be 0, 1, 25, 100 and 200 μM. Cd solutions were prepared by dissolving analytical-grade $CdCl_2$ in sterilized BG-11 medium at the desired concentrations just before the experiment. The samples without Cd were used as the control. During the whole experiment, all the samples were cultured under fluorescent white light (30 μmol photons $m^{-2}\,s^{-1}$) with a 12:12 h light–dark cycle at 24 ± 2 °C. The measurements were carried out at 0, 6, 12, 24, 48, 72 and 96 h after onset of different treatments.

2.3. Measurement of O_2 evolution and respiratory O_2 consumption

After the cells were exposed to various concentrations of Cd for different time, 2 mL of cells were added into the reaction cuvette of a Clark-type oxygen electrode (Oxygraph, Hansatech Instruments Ltd., King's Lynn, Norfolk, England). A white light provided illumination on the surface of the cuvette at about 400 μmol photons $m^{-2}\,s^{-1}$ during the measurement of O_2 evolution rate in the light (nmol $mL^{-1}\,min^{-1}$), which reached its stable ratio within 5 min. Then the cuvette was kept in darkness to detect the respiratory O_2 consumption rate in the dark (nmol $mL^{-1}\,min^{-1}$). The sum of O_2 evolution rate in the light and the respiratory O_2 consumption rate in the dark was calculated as net O_2 evolution rate (nmol $mL^{-1}\,min^{-1}$).

2.4. Transmission electron microscopy (TEM)

For transmission electron microscopy (TEM), algal cells were harvested by centrifugation (4000*g*, 5 min) after the cells were exposed to various concentration of Cd for 96 h. Algal cells were rinsed with culture medium for a short time and subsequently washed in glutaraldehyde in 0.1 M phosphate buffer (pH 7.3). Then the cells were fixed for 24 h in 0.1 M phosphate buffer containing 2% glutaraldehyde. The fixed cells were centrifuged, re-suspended and rinsed several times in 0.1 M sodium cacodylate buffer containing sucrose. The algal cells were post-fixed with 2% osmium tetroxide. The cells were dehydrated in a graded acetone series after centrifugation and embedded in Epon 812 (Nishikawa and Tominaga, 2001). Ultrathin sections were stained with 1% uranyl acetate and lead citrate. Ultrastructure of cells was observed with a transmission electron microscope (SU080, Hitach, Japan).

2.5. Measurement of activities of the photosystems

2.5.1. Application of the Dual-PAM-100 system

The activities of PSI and PSII were measured with a Dual-PAM-100 system (Heinz Walz GmbH, Effeltrich, Germany). The cells used for measurements were injected into the DUAL-K25 quartz glass cuvette. The quartz glass cuvette was then sandwiched between the emitter head and detector head of the system. All the samples were dark-adapted for 5 min before measurement.

2.5.2. Measurement of the slow induction curve

The measurements were performed using the automated induction program provided by the Dual-PAM software (Pfündel et al., 2008) with a slight modification. After the samples were dark-adapted for 5 min, the minimal fluorescence after dark-adaptation, F_0, was detected by a measuring light at low intensity. A saturating pulse with duration of 300 ms and a light intensity of 10000 μmol photons $m^{-2}\,s^{-1}$ was then applied to detect the maximum fluorescence after dark-adaptation, F_m. The maximal change in $P700^+$ signal, P_m, was determined through the application of a saturation pulse after far-red pre-illumination for 10 s according to the methods of Klughammer and Schreiber (1994, 2008b).

After the determination of F_0, F_m and P_m, the slow induction curve was recorded with the routine of the Dual-PAM software. The actinic light was applied at the intensity of 30 μmol $m^{-2}\,s^{-1}$, as same as the light intensity at which the algae cells were cultured. The slow induction curve was used in the analysis of photosynthesis under light. A saturating pulse with duration of 300 ms was applied every 20 s after the onset of the actinic light to determine the maximum fluorescence signal (F'_m) and maximum $P700^+$ signal (P'_m) under the actinic light. The slow induction curve was recorded for 120 s to achieve the steady state of the photosynthetic apparatus, and then the actinic light was turned off. The data derived after the final saturating pulse was used in the analysis of the activities of PSI, PSII and CEF based on previously determined F_0, F_m and P_m.

2.5.3. Quantum yields of the photosystems and CEF

The quantum yields of PSI and PSII were detected by saturating pulses during the process of slow induction curve and calculated automatically by the Dual-PAM software. The quantum yields of energy conversion in PSII were calculated according to the method of Kramer et al. (2004), which can be transformed into the following simpler equations (Klughammer and Schreiber, 2008a; Suzuki et al., 2011):

$$Y(II) = (F'_m - F)/F'_m \quad (1)$$

$$Y(NPQ) = F/F'_m - F/F_m \quad (2)$$

$$Y(NO) = F/F_m \quad (3)$$

where F was the steady state fluorescence, Y(II) was the effective photochemical quantum yield of PSII, Y(NPQ) was the quantum yield of light-induced non-photochemical fluorescence quenching, and Y(NO) was the quantum yield of non-light-induced non-photochemical fluorescence quenching.

The quantum yields of energy conversion in PSI were calculated according to Klughammer and Schreiber (2008b) and Suzuki et al. (2011):

$$Y(I) = (P'_m)/P_m \quad (4)$$

$$Y(ND) = (P - P_0)/P_m \quad (5)$$

$$Y(NA) = (P_m - P'_m)/P_m \quad (6)$$

where Y(I) was effective photochemical quantum yield of PSI, Y(ND) was the quantum yield of non-photochemical energy dissipation in reaction centers due to donor side limitation, Y(NA) was the quantum yield of non-photochemical energy dissipation of reaction centers due to acceptor side limitation. The $P700^+$ signal (P) was recorded just before a saturation pulse. Then a saturation pulse was applied to determine maximum $P700^+$ signal (P'_m). The minimum level of the $P700^+$ signal (P_0) was detected at a 1 s dark interval after each saturation pulse. The signals P and P'_m were detected referenced against P_0.

The quantum yield of CEF was calculated from the difference between Y(I) and Y(II) (Huang et al., 2010):

$$Y(CEF) = Y(I) - Y(II) \quad (7)$$

2.5.4. The electron transport rates in PSI and PSII

Electron transport rates (ETRs) in PSI and PSII, i.e. ETR(I) and ETR(II), were recorded during the measurement of the slow induction curve and defined and calculated automatically by the Dual-PAM software as follows (Maxwell and Johnson, 2000; Suzuki et al., 2011):

$$ETR(I) = Y(I) \times PAR \times 0.84 \times 0.5 \quad (8)$$

$$ETR(II) = Y(II) \times PAR \times 0.84 \times 0.5 \quad (9)$$

2.5.5. Relation between cyclic electron flow (CEF) and linear electron flow (LEF)

The relation between cyclic electron flow (CEF) and linear electron flow (LEF) was detected by calculating the changes of the ratios of Y(CEF)/Y(I), Y(CEF)/Y(II) and Y(II)/Y(I). The ratios of Y(CEF)/Y(I) and Y(II)/Y(I) indicated the contribution of CEF and LEF to the yield of PSI. The ratio of Y(II)/Y(I) also showed the distribution of quantum yield between two photosystems. Y(CEF)/Y(II) indicated the ratio of quantum yield of CEF to that of LEF (Huang et al., 2010).

2.6. Statistics

Each treatment was replicated four times. Means and standard deviation (S.D.) were calculated and presented. The statistical significance of differences between treatments and control was determined using Student's t-test and was accepted when P value was less than 0.05.

3. Results

3.1. Effects of Cd on O_2 evolution and respiratory O_2 consumption

Net O_2 evolution rates (based on per mL per min) of the cells treated with 0, 1 and 25 μM Cd increased during the experiment (0–96 h). However, the net O_2 evolution rates of the cells treated with 100 μM Cd did not show obvious increase during the experiment. The value of net O_2 evolution rate decreased at 200 μM Cd. After 12 h of exposure to Cd, net O_2 evolution rates of the cells treated with 25, 100 and 200 μM Cd began to show significant difference compared to control. The activity of O_2 evolution

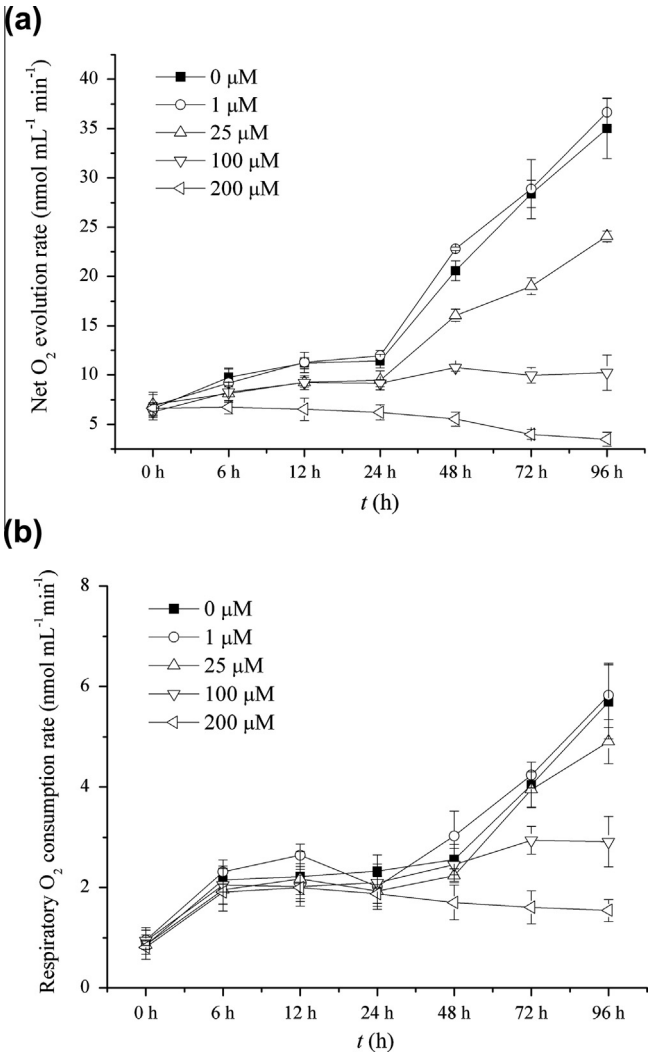

Fig. 1. Effects of Cd on O_2 evolution and respiratory O_2 consumption. (a) O_2 evolution rate (nmol mL^{-1} min^{-1}), which was calculated as the sum of O_2 evolution rate in the light and the respiratory O_2 consumption rate in the dark. (b) The respiratory O_2 consumption rate (nmol mL^{-1} min^{-1}) in the dark. Data were means ± S.D. (n = 4).

significantly decreased when the cells were treated with 25, 100 and 200 μM Cd for 96 h compared to that of control (Fig. 1a).

Respiratory O_2 consumption rates of the cells in all treatments increased in the beginning 12 h. The respiratory O_2 consumption rates of cells treated with 0, 1 and 25 μM Cd kept increasing after 24 h, while respiratory O_2 consumption rates showed no obvious increase at 100 μM or even decreased at 200 μM. Respiratory O_2 consumption rates began to show significant difference between Cd treatments and control after 72 h. The respiratory activity significantly decreased when the cells were treated with 100 and 200 μM Cd for 72 h and thereafter in comparison with the control (Fig. 1b).

3.2. Effects of Cd on the ultrastructure of C. pyrenoidosa cells

The ultrastructure of algal cells treated with 200 μM Cd for 96 h was comparatively analyzed with the control (Fig. 2). Fig. 2a showed the ultrastructure of cells without Cd exposure. The different organelle compartment was easily distinguished. The chloroplast, well ordered thylakoids and different layers of cell wall were intact and clearly observed (Fig. 2a). On the contrary, some cells were significant damaged, showing the toxic effects of Cd on alga cells (Fig. 2b). Comparing to the ultrastructure of control cells, the cytoplasm became heterospheric, and cytoplasmic vacuolization and appearance of various types of vacuoles could be observed in some Cd-treated cells. Although some cells treated with Cd still show the structure of chloroplasand thylakoids, most organelle were altered by Cd toxicity. Cd also showed modifications on the cell wall structure.

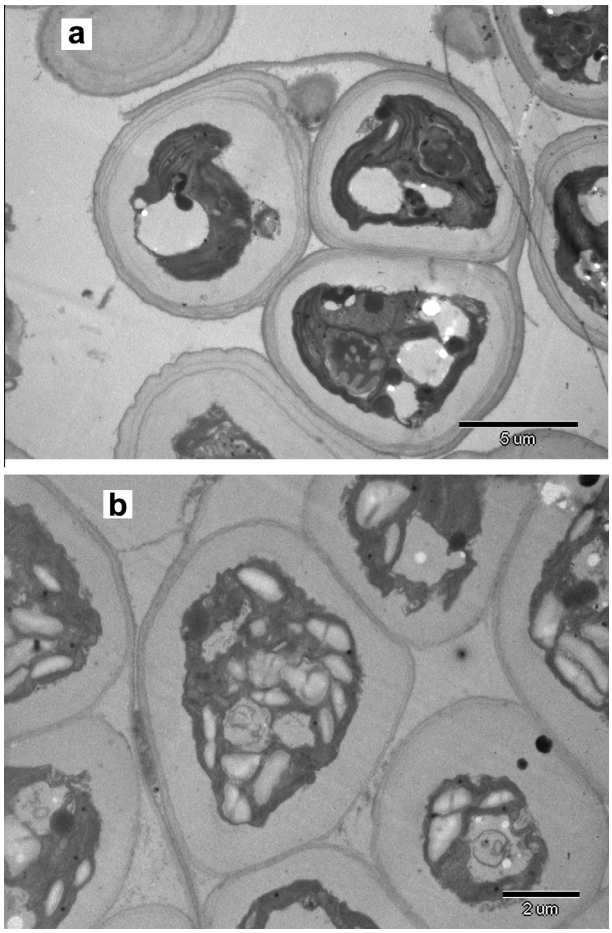

Fig. 2. The ultrastructure of algae cells detected by transmission electron microscopy (TEM). (a) Cells treated with 0 μM Cd (control) (×12000). (b) Cells treated with 200 μM Cd (×15000). Cell structure was obviously damaged, showing the toxic effects of Cd on algal cells. The measurement was carried out after the cells were exposure to various concentrations of Cd for 96 h.

3.3. Effects of Cd on Y(I), Y(II) and Y(CEF)

Y(I) did not show significant difference between different treatments and the control during the experiment (0–96 h) except that Y(I) significantly decreased when treated by 200 μM Cd for 96 h (Fig. 3a). The value of Y(II) was less than Y(I) and decreased with increasing Cd concentration. After exposure to Cd for 12 h, Y(II) of the treatments with 25, 100 and 200 μM Cd began to show significant difference compared to control. The value of Y(II) of the cells treated with 200 μM Cd gradually decreased during the experiment and was only half of that of control after 96 h (Fig. 3b). Y(CEF) increased slightly when treated with Cd and was much higher than the control when the cells were treated with 200 μM Cd for more than 72 h (Fig. 3c).

3.4. Effects of Cd on ETR(I) and ETR(II)

ETR(I) maintained steady value when the cells were treated with 0, 1, 25 and 100 μM Cd. However, the electron transport in PSI was inhibited after the cells were exposure to 200 μM Cd for 96 h, indicated by the significant decrease of ETR(I) compared to the control (Fig. 4). ETR(II) was lower than ETR(I) in *C. pyrenoidosa*. ETR(II) decreased with increasing Cd concentration after exposure for 96 h. After exposure to 200 μM Cd for 96 h, ETR(II) was only half of that of control (Fig. 4).

3.5. Changes of the relation between CEF and LEF

The ratio of Y(CEF)/Y(I), Y(CEF)/Y(II) increased, and the ratio of Y(II)/Y(I) decreased with increasing concentration of Cd (Fig. 5). Because Y(I) kept relatively steady and Y(II) significantly decreased with increasing concentration of Cd, the ratio of Y(II)/Y(I) decreased with increasing concentration of Cd after 96 h. The contribution of CEF to Y(I) increased with increasing Cd concentration, indicated by the increase of the ratio of Y(CEF)/Y(I) of Cd (Fig. 5). The relation between CEF and LEF could also be derived from the change of the ratio of Y(CEF)/Y(II). Y(CEF)/Y(II) significantly increased due to the treatment of Cd. After exposure to 200 μM Cd for 96 h, the quantum yield of CEF was more than twice of that of LEF, which led to the increase of the ratio of Y(CEF)/Y(II) from 0.8 of the control to 2.2 of the treatment with 200 μM Cd (Fig. 5).

3.6. Changes of complementary quantum yields of energy conversion in PSI and PSII

Values of photochemical quantum yields of PSI and PSII had been shown in Fig. 3. The changes of Y(I) and Y(II) after treated by Cd for 96 h were also compared with the changes of Y(NA), Y(ND), Y(NO) and Y(NPQ) to detect the effects of Cd on the complementary quantum yields of energy conversion in PSI and PSII (Table 1).

Although Y(I) showed significant decrease when treated by 200 μM Cd, the value of Y(I) still kept 93% to that of control. Y(I) did not show significant difference between treatments with 0, 1, 25, 100 μM Cd. Y(ND) significantly increased due to treatment of 200 μM Cd but showed no significant change in other treatments. Y(NA) showed no significant difference between treatments and control. As for the complementary quantum yields of energy conversion in PSII, Y(II) significantly decreased when the cells were treated with 100 and 200 μM Cd. Y(NO) significantly increased when the cells were exposed to 100 and 200 μM Cd for 96 h.

Y(NPQ) significantly decreased due to the treatment of 200 μM Cd but showed no significant change in other treatments.

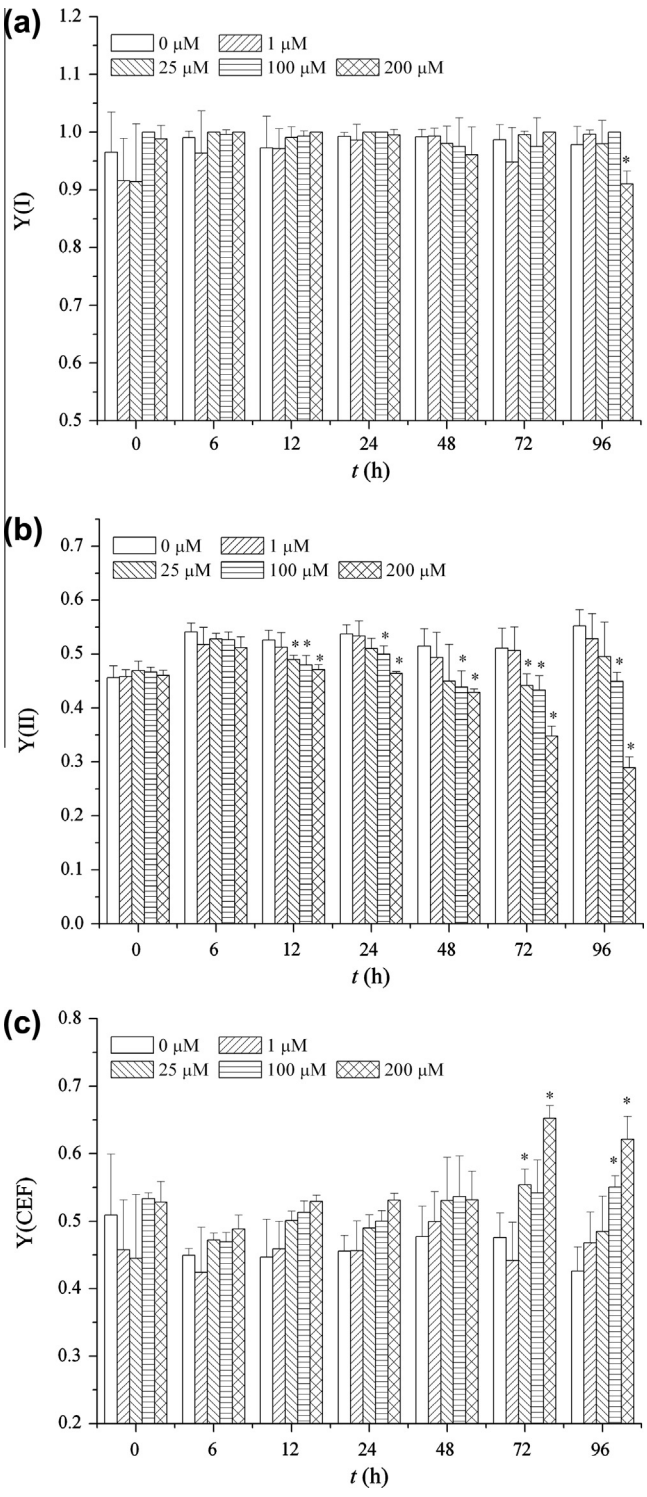

Fig. 3. The quantum yields of PSI, PSII and CEF. (a) Y(I), the photochemical quantum yield of PSI. (b) Y(II), the photochemical quantum yield of PSII. (c), Y(CEF), the quantum yield of cyclic electron flow (CEF). Measurements were carried out at 0, 6, 12, 24, 48, 72 and 96 h after exposure to various concentrations of Cd. Data were detected from the slow induction curve, where the actinic light was supplied at the intensity of 30 μmol m^{-2} s^{-1} and last for 120 s. The data derived from the final saturating pulse was used in the analysis and shown. Data were means ± S.D. (n = 4) and significant levels between control and treatments were indicated by asterisks (P < 0.05).

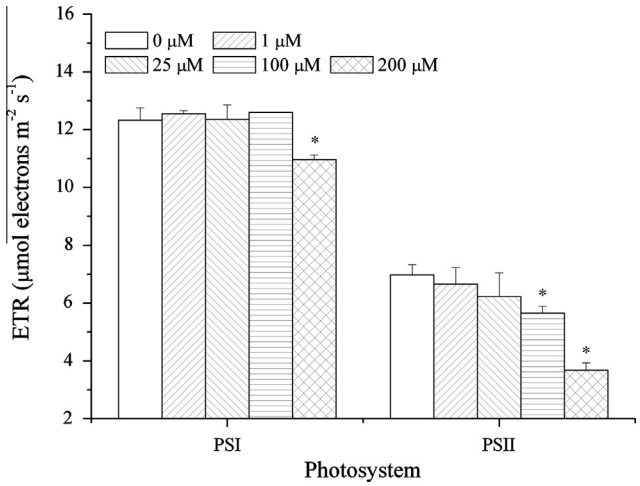

Fig. 4. The electron transport rates in PSI and PSII. Measurements were carried out after the cells were exposed to various concentrations of Cd for 96 h. Data were derived from the final saturating pulse of the slow induction curve. Data were means ± S.D. (n = 4) and significant levels between control and treatments were indicated by asterisks (P < 0.05).

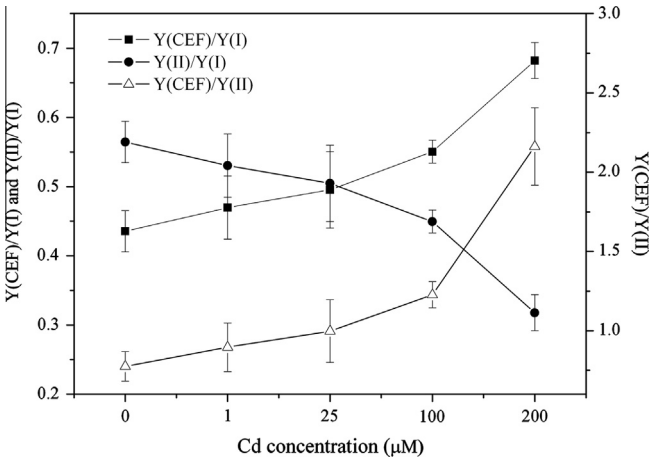

Fig. 5. The ratios of Y(CEF)/Y(I), Y(CEF)/Y(II) and Y(II)/Y(I). These ratios were calculated from the value of Y(I), Y(II) and Y(CEF) after exposure to various concentrations of Cd for 96 h. Y(CEF)/Y(I) and Y(II)/Y(I) indicated the contribution of cyclic electron flow (CEF) and linear electron flow (LEF) to the yield of PSI. The ratio of Y(II)/Y(I) also showed the distribution of quantum yield between two photosystems. Y(CEF)/Y(II) indicated the ratio of quantum yield of CEF to that of LEF. All the data presented here were calculated from four duplications.

3.7. The correlations between Y(II), Y(NO) and Y(CEF)

The changes of Y(II), Y(NO) and Y(CEF) after exposure to various concentrations of $CdCl_2$ for 96 h were shown in Fig. 6. Y(NO) was negatively correlated with Y(II) (Fig. 6a), but positively correlated with Y(CEF) (Fig. 6c). There was a significant negative correlation between Y(II) and Y(CEF) (Fig. 6b).

4. Discussion

In the present study, toxic effects of Cd on the cell structure of *C. pyrenoidosa*, photosynthetic oxygen development and respiration, activities of PSI, PSII and CEF were examined. The quantum yields of PSI, PSII and CEF, the electron transport and energy dissipation of PSI and PSII, and the relation between PSI and PSII under Cd treatment were analyzed.

Table 1
The complementary quantum yields of energy conversion in PSI and PSII.

Concentration of Cd (μM)	Quantum yields in PSI			Quantum yields in PSII		
	Y(I)	Y(ND)	Y(NA)	Y(II)	Y(NO)	Y(NPQ)
0	0.978 ± 0.032	0.000 ± 0.000	0.022 ± 0.032	0.552 ± 0.030	0.409 ± 0.026	0.039 ± 0.006
1	0.997 ± 0.007	0.011 ± 0.021	0.000 ± 0.000	0.529 ± 0.046	0.439 ± 0.043	0.032 ± 0.004
25	0.980 ± 0.041	0.000 ± 0.000	0.020 ± 0.041	0.495 ± 0.064	0.480 ± 0.067	0.025 ± 0.011
100	1.000 ± 0.000	0.000 ± 0.000	0.000 ± 0.000	0.450 ± 0.017*	0.519 ± 0.014*	0.032 ± 0.009
200	0.910 ± 0.023*	0.080 ± 0.015*	0.010 ± 0.008	0.289 ± 0.020*	0.705 ± 0.014*	0.007 ± 0.013*

Data were detected from the slow induction curve after exposure to various concentrations of Cd for 96 h. The data derived from the final saturating pulse were used in the analysis. Data were means ± S.D. ($n = 4$) and significant levels between treatments and control were indicated by asterisks ($P < 0.05$).

Cd is passively absorbed by organisms and its toxicity is concentration-dependent (Das et al., 1997; Kola and Wilkinson, 2005). The present study showed that the toxicity of Cd increased with its increasing concentration. Cd causes inhibition or inactivation of many enzymes mainly by its binding to functional groups and thus shows inhibition of the growth, photosynthesis or respiration in plant cells and algae (Tukaj et al., 2007; Baścik-Remisiewicz et al., 2009). There are antagonisms between Ca or Mn and Cd. Detoxifying role of Ca or Mn had been reported in some previous studies (Pellegrini et al., 1993; Baścik-Remisiewicz et al., 2009) and the protective role of Ca is confirmed by cytological observations (Pellegrini et al., 1993).

Cd inhibited the activities of photosynthetic oxygen development and respiration (Fig. 1). It was reported that Cd seriously inhibited oxygen evolution (Tukaj et al., 2007) and caused the disassembly of PSII (Atal et al., 1991).

Silverberg (1976) found that exposure of three species of green algae to $CdCl_2$ resulted in the formation of intramitochondrial granules containing cadmium and the inhibition of some functional activities within mitochondria with the modification of their structure. The modification of structure and functional activities of mitochondria was in accordance with the inhibition of respiratory O_2 consumption rate (Fig. 1b). The most striking modifications were modification of cell wall, cytoplasmic vacuolization and the degradation of chloroplast. These results suggest the localization of Cd in the cells and the role of cell wall and vacuole in conferring metal tolerance (Aguilera and Amils, 2005; Kola and Wilkinson, 2005).

In the present study, treatment with Cd was applied at higher concentrations than those found in the real environment, but such treatments can be used to provide the data on the acute toxicity of Cd on the physiological activity of *C. pyrenoidosa*. The lowest concentration (1 μM) used in the experiment had no effect on oxygen evolution, respiration and PSI activity, indicating the Cd tolerance of the microalga strain.

Y(I) kept almost to 1 during the whole experiment (0–96 h), indicating the stability of the activity of PSI. As shown in some other studies, PSI showed the ability to maintain physiological activity under environmental stress (Li et al., 2006; Huang et al., 2010). The activity of PSI was also shown to be stable when the algae cells were treated with Cd less than 100 μM. These results showed the tolerance of PSI to Cd exposure. On the contrary, PSII was more susceptible to Cd treatment, as shown by the significant decrease of Y(II) with increasing Cd concentration (Fig. 3b). Many studies demonstrated that PSII was one of the most sensitive target sites for environmental stress, such as low temperature (Pan et al., 2009; Huang et al., 2010), high temperature (Yamane et al., 1997; Lípová et al., 2010), and heavy metals (Qian et al., 2009; Zhang et al., 2010). In the present study, Y(II) of the cells treated with 200 μM Cd gradually decreased during the experiment, indicating that the treatment with high concentration of Cd (200 μM) significantly inhibited PSII activity. Exposure to 100 μM Cd had no inhibition on Y(I) whereas Y(II) showed significant decrease compared to the control. The Dual-PAM-100 system, which could test the activities of PSI and PSII simultaneously, provides useful information about the effects of contaminants such as heavy metals on the photosynthetic apparatus. The simultaneous test of the activities of PSI and PSII confirmed the conclusion of some previous studies that PSII was more sensitive than PSI to some environmental stress (Qian et al., 2009; Lípová et al., 2010).

CEF was stimulated when the cells were treated with $CdCl_2$, indicated by the increase of Y(CEF) with increasing Cd concentration (Fig. 3c). This implies the activating effect of heavy metal such as Cd on CEF. CEF have been found to be stimulated under some other stressful conditions (Huang et al., 2010; Gao and Wang, 2012). Y(II) significantly decreased due to Cd treatment. However, Y(I) could still have the ability to keep its stability because Y(CEF) made important contribution to the stability of Y(I) under Cd treatment. The contribution of Y(CEF) to Y(I) could also be found from the change of the ratio of Y(CEF)/Y(I) under Cd treatment. These results confirmed that the activation of CEF around PSI played an important role in protecting PSI from toxicity of Cd, which had been suggested in some previous studies (Zhou et al., 2006; Qian et al., 2009). The activation of CEF also enhanced the stability of ETR(I) (Fig. 4).

LEF made big contribution to the yield of PSI in the untreated cells but decreased due to Cd treatment. The contribution of CEF to the yield of PSI increased with the increasing Cd concentration. It has been reported that inhibition of LEF and stimulation of CEF around PSI are two main mechanisms for the photoprotection of PSI (Munekage et al., 2002; Huang et al., 2010). This study suggests that these mechanisms exist in the protection of PSI under Cd stress.

The stability of the activity of PSI was associated with the low value of Y(NA) and Y(ND), which indicated that there was almost no donor and acceptor side limitation of PSI (Table 1). The value of Y(NA) was almost zero after exposure to different concentration of Cd for 96 h mainly due to the activation of CEF under the treatment of Cd. These results were in agreement with some previous studies that CEF was stimulated as an important mechanism for preventing acceptor side limitation of PSI (Munekage et al., 2002; Huang et al., 2012).

CEF is also suggested to play an important role in the activation of NPQ and the synthesis of more ATP needed for the repair of photosynthetic apparatus under environmental stress (Johnson, 2011; Huang et al., 2012). When the cells were treated with Cd, the activation of CEF was helpful for the induction of NPQ under 1, 25, 100 μM Cd. These were shown by Y(NPQ) (Table 1). However, because of the serious toxicity of high concentration of Cd (200 μM), Y(II) significantly decreased and the cells began to lose the activation of NPQ (Table 1). The loss of the activation of NPQ indicated its failure to protect the photosynthetic apparatus under such high concentration of Cd (200 μM).

The significant decrease of Y(II) after exposure to 100 and 200 μM Cd for 96 h indicated that t reatment with high concentration of Cd caused damage to PSII. The decrease of Y(II) were due to

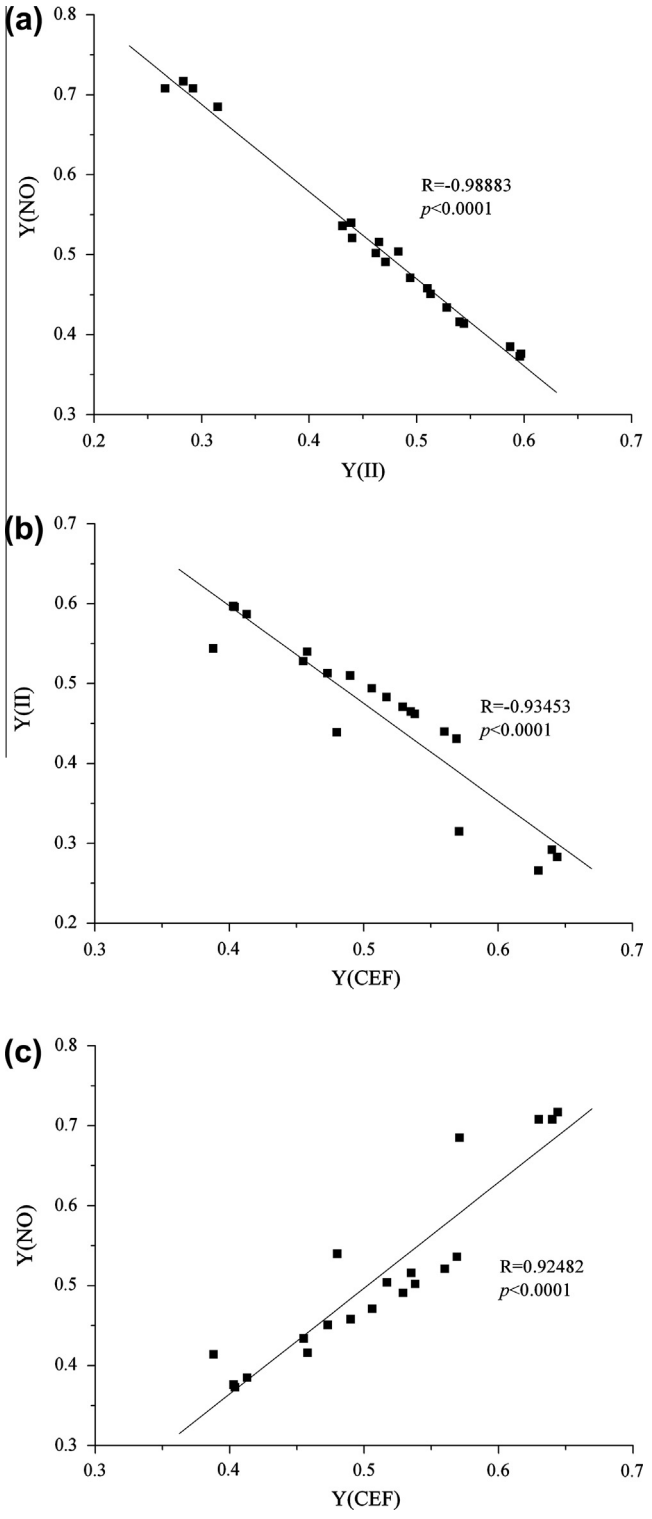

Fig. 6. The correlations between Y(II), Y(NO) and Y(CEF). (a) The correlation between Y(II) and Y(NO). (b) The correlation between Y(II) and Y(CEF). (c) The correlation between Y(CEF) and Y(NO). Data were derived from the final saturating pulse of the slow induction curve after exposure to various concentrations of Cd for 96 h. All the data presented here were calculated from 20 measurements.

the increase of Y(NO), the quantum yield of non-light-induced non-photochemical fluorescence quenching (Table 1). Y(NO) was negatively correlated with Y(II) (Fig. 6a), suggesting that Y(NO) was also a good indicator of PSII damage (Huang et al., 2010). In the present study, a significant positive correlation between the extent of PSII damage and stimulation of CEF was found when treated with Cd, indicated by the positive correlation between Y(NO) and Y(CEF) (Fig. 6c). Together with the negative correlation between Y(II) and Y(CEF), these results indicated that the demand for synthesis of ATP in repair increased with increasing Cd concentration. The demand for synthesis of ATP increased as the damage increased. When the cells were treated with Cd, extra ATP could be provided with the help of the stimulation of CEF (Huang et al., 2010, 2012; Johnson, 2011).

5. Conclusions

Cd treatment showed inhibitory effects on physiological activities of *C. pyrenoidosa* at several sites: impairment of the chloroplast structure and its function, cytoplasmic vacuolization, modifications of cell wall structure, inhibition of activities of oxygen evolution and respiration, and quantum yield and electron transport in PSI and PSII. Oxygen evolution activity was sensitive to Cd treatment and seriously inhibited by 100 and 200 μM Cd. Cd treatment showed significant inhibitory effect on the PSII activity while PSI was tolerant to Cd at less than 100 μM. The decrease of Y(II) were due to the increase of Y(NO), and these change indicate the dysfunction of PSII. ETR(II) significantly decreased with increasing Cd concentration after 96 h. LEF made big contribution to the photochemical quantum yield of PSI in the untreated cells but decreased with increasing Cd concentration. The contribution of CEF to the yield of PSI increased with increasing Cd concentration. CEF was stimulated as an important mechanism for preventing acceptor side limitation of PSI and played an essential role for protection of PSI. The activation of CEF enhanced the tolerance of Y(I) and ETR(I) to Cd treatment.

Acknowledgements

This work was supported by Program of 100 Distinguished Young Scientists of the Chinese Academy of Sciences and National Natural Science Foundation of China (U1120302 and 21177127).

References

Aguilera, A., Amils, R., 2005. Tolerance to cadmium in *Chlamydomonas* sp. (Chlorophyta) strains isolated from an extreme acidic environment, the Tinto River (SW, Spain). Aquat. Toxicol. 75, 316–329.

Appenroth, K.J., Stöckel, J., Srivastava, A., Strasser, R.J., 2001. Multiple effects of chromate on the photosynthetic apparatus of *Spirodela polyrhiza* as probed by OJIP chlorophyll *a* fluorescence measurements. Environ. Pollut. 115, 49–64.

Atal, N., Saradhi, P.P., Mohanty, P., 1991. Inhibition of the chloroplast photochemical reactions by treatment of wheat seedlings with low concentrations of cadmium: analysis of electron transport activities and changes in fluorescence yield. Plant Cell Physiol. 32, 943–951.

Baścik-Remisiewicz, A., Tomaszewska, E., Labuda, K., Tukaj, Z., 2009. The effect of Zn and Mn on the toxicity of Cd to the green microalga *Desmodesmus armatus* cultured at ambient and elevated (2%) CO_2 concentrations. Polish J. Environ. Stud. 18, 775–780.

Chen, Z., Ren, L., Shao, Q., Shi, D., Ru, B., 1999. Expression of mammalian metallothionein-I gene in cyanobacteria to enhance heavy metal resistance. Mar. Pollut. Bull. 39, 155–158.

Coopman, R.E., Fuentes-Neira, F.P., Briceño, V.F., Cabrera, H.M., Corcuera, L.J., Bravo, L.A., 2010. Light energy partitioning in photosystems I and II during development of *Nothofagus nitida* growing under different light environments in the Chilean evergreen temperate rain forest. Trees Struct. Funct. 24, 247–259.

Das, P., Samantaray, S., Rout, G.R., 1997. Studies on cadmium toxicity in plants: a review. Environ. Pollut. 98, 29–36.

Dewez, D., Geoffroy, L., Vernet, G., Popovic, R., 2005. Determination of photosynthetic and enzymatic biomarkers sensitivity used to evaluate toxic effects of copper and fludioxonil in alga *Scenedesmus obliquus*. Aquat. Toxicol. 74, 150–159.

Fargašová, A., Bumbálová, A., Havránek, E., 1999. Ecotoxicological effects and uptake of metals (Cu^{+}, Cu^{2+}, Mn^{2+}, Mo^{6+}, Ni^{2+}, V^{5+}) in freshwater alga *Scenedesmus quadricauda*. Chemosphere 38, 1165–1173.

Gao, S., Wang, G., 2012. The enhancement of cyclic electron flow around photosystem I improves the recovery of severely desiccated *Porphyra yezoensis* (Bangiales, Rhodophyta). J. Exp. Bot. 63, 4349–4358.

Huang, W., Yang, S.J., Zhang, S.B., Zhang, J.L., Cao, K.F., 2012. Cyclic electron flow plays an important role in photoprotection for the resurrection plant *Paraboea rufescens* under drought stress. Planta 235, 819–828.

Huang, W., Zhang, S.B., Cao, K.F., 2010. Stimulation of cyclic electron flow during recovery after chilling-induced photoinhibition of PSII. Plant Cell Physiol. 51, 1922–1928.

Johnson, G.N., 2011. Reprint of: Physiology of PSI cyclic electron transport in higher plants. Biochim. Biophys. Acta Bioenerg. 1807, 906–911.

Khattar, J.I.S., Shailza, 2009. Optimization of Cd^{2+} removal by the cyanobacterium *Synechocystis pevalekii* using the response surface methodology. Process Biochem. 44, 118–121.

Klughammer, C., Schreiber, U., 1994. An improved method, using saturating light pulses, for the determination of photosystem I quantum yield via $P700^{+}$-absorbance changes at 830 nm. Planta 192, 261–268.

Klughammer, C., Schreiber, U., 2008a. Complementary PS II quantum yields calculated from simple fluorescence parameters measured by PAM fluorometry and the Saturation Pulse method. PAM Appl. Notes 1, 27–35.

Klughammer, C., Schreiber, U., 2008b. Saturation Pulse method for assessment of energy conversion in PS I. PAM Appl. Notes 1, 11–14.

Kola, H., Wilkinson, K.J., 2005. Cadmium uptake by a green alga can be predicted by equilibrium modelling. Environ. Sci. Technol. 39, 3040–3047.

Kramer, D.M., Johnson, G., Kiirats, O., Edwards, G.E., 2004. New fluorescence parameters for the determination of QA redox state and excitation energy fluxes. Photosynth. Res. 79, 209–218.

Lípová, L., Krchňák, P., Komenda, J., Ilík, P., 2010. Heat-induced disassembly and degradation of chlorophyll-containing protein complexes in vivo. Biochim. Biophys. Acta 1797, 63–70.

Li, X.G., Zhao, J.P., Xu, P.L., Meng, J.J., He, Q.W., 2006. Effects of cyclic electron flow inhibitor (antimycin A) on photosystem photoinhibition of sweet pepper leaves upon exposure to chilling stress under low irradiance. Agric. Sci. China 5, 506–511.

Maxwell, K., Johnson, G.N., 2000. Chlorophyll fluorescence – a practical guide. J. Exp. Bot. 51, 659–668.

Monteiro, C.M., Fonseca, S.C., Castro, P.M.L., Malcata, F.X., 2011. Toxicity of cadmium and zinc on two microalgae, *Scenedesmus obliquus* and *Desmodesmus pleiomorphus*, from Northern Portugal. J. Appl. Phycol. 23, 97–103.

Munekage, Y., Hashimoto, M., Miyake, C., Tomizawa, K.-I., Endo, T., Tasaka, M., Shikanai, T., 2004. Cyclic electron flow around photosystem I is essential for photosynthesis. Nature 429, 579–582.

Munekage, Y., Hojo, M., Meurer, J., Endo, T., Tasaka, M., Shikanai, T., 2002. *PGR5* is involved in cyclic electron flow around Photosystem I and is essential for photoprotection in *Arabidopsis*. Cell 110, 361–371.

Nawrot, T., Plusquin, M., Hogervorst, J., Roels, H.A., Celis, H., Thijs, L., Vangronsveld, J., Van Hecke, E., Staessen, J.A., 2006. Environmental exposure to cadmium and risk of cancer: a prospective population-based study. Lancet Oncol. 7, 119–126.

Neelam, A., Rai, L.C., 2003. Differential responses of three cyanobacteria to UV-B and Cd. J. Microbiol. Biotechnol. 13, 544–551.

Nishikawa, K., Tominaga, N., 2001. Isolation, growth, ultrastructure, and metal tolerance of the green alga, *Chlamydomonas acidophila* (Chlorophyta). Biosci. Biotechnol. Biochem. 65, 2650–2656.

Pan, X.L., Zhang, D.Y., Chen, X., Li, L., Mu, G.J., Li, L.H., Bao, A.M., Liu, J., Zhu, H.S., Song, W.J., Yang, J.Y., Ai, J.Y., 2009. Effects of short-term low temperatures on photosystem II function of samara and leaf of Siberian maple (*Acer ginnala*) and subsequent recovery. J. Arid Land 1, 57–63.

Pellegrini, M., Laugier, A., Sergent, M., Phan-Tan-Luu, R., Valls, R., Pellegrini, L., 1993. Interactions between the toxicity of the heavy metals cadmium, copper, zinc in combinations and the detoxifying role of calcium in the brown alga *Cystoseira barbata*. J. Appl. Phycol. 5, 351–361.

Perales-Vela, H.V., González-Moreno, S., Montes-Horcasitas, C., Cañizares-Villanueva, R.O., 2007. Growth, photosynthetic and respiratory responses to sub-lethal copper concentrations in *Scenedesmus incrassatulus* (Chlorophyceae). Chemosphere 67, 2274–2281.

Pfündel, E., Klughammer, C., Schreiber, U., 2008. Monitoring the effects of reduced PS II antenna size on quantum yields of photosystems I and II using the Dual-PAM-100 measuring system. PAM Appl. Notes 1, 21–24.

Qian, H.F., Li, J.J., Sun, L.W., Chen, W., Sheng, G.D., Liu, W.P., Fu, Z.W., 2009. Combined effect of copper and cadmium on *Chlorella vulgaris* growth and photosynthesis-related gene transcription. Aquat. Toxicol. 94, 56–61.

Siedlecka, A., Krupa, Z., 1996. Interaction between cadmium and iron and its effects on photosynthetic capacity of primary leaves of *Phaseolus vulgaris*. Plant Physiol. Biochem. 34, 833–841.

Silverberg, B.A., 1976. Cadmium-induced ultrastructural changes in mitochondria of freshwater green algae. Phycologia 15, 155–159.

Stanier, R., Kunisawa, R., Mandel, M., Cohen-Bazire, G., 1971. Purification and properties of unicellular blue-green algae (order *Chroococcales*). Bacteriological Rev. 35, 171–205.

Suzuki, K., Ohmori, Y., Ratel, E., 2011. High root temperature blocks both linear and cyclic electron transport in the dark during chilling of the leaves of rice seedlings. Plant Cell Physiol. 52, 1697–1707.

Tukaj, Z., Baścik-Remisiewicz, A., Skowroński, T., Tukaj, C., 2007. Cadmium effect on the growth, photosynthesis, ultrastructure and phytochelatin content of green microalga *Scenedesmus armatus*: a study at low and elevated CO_2 concentration. Environ. Exp. Bot. 60, 291–299.

Wang, J.L., Chen, C., 2009. Biosorbents for heavy metals removal and their future. Biotechnol. Adv. 27, 195–226.

Wang, S.Z., Pan, X.L., 2012. Effects of Sb(V) on growth and chlorophyll fluorescence of *Microcystis aeruginosa* (FACHB-905). Curr. Microbiol. 65, 733–741.

Yamane, Y., Kashino, Y., Koike, H., Satoh, K., 1997. Increases in the fluorescence F_o level and reversible inhibition of Photosystem II reaction center by high-temperature treatments in higher plants. Photosynth. Res. 52, 57–64.

Zhang, D.Y., Pan, X.L., Mu, G.J., Wang, J.L., 2010. Toxic effects of antimony on photosystem II of *Synechocystis* sp. as probed by in vivo chlorophyll fluorescence. J. Appl. Phycol. 22, 479–488.

Zhou, W., Juneau, P., Qiu, B., 2006. Growth and photosynthetic responses of the bloom-forming cyanobacterium *Microcystis aeruginosa* to elevated levels of cadmium. Chemosphere 65, 1738–1746.